AD-A049 681 WASHINGTON UNIV SEATTLE DEPT OF MECHANICAL ENGINEERING F/G 11/9
DYNAMIC PHOTOELASTICITY AND DYNAMIC FINITE ELEMENT ANALYSES OF --ETC(U)
JAN 78 S MALL, A S KOBAYASHI, Y URABE N00014-76-C-0060
UNCLASSIFIED TR-32 NL

| OF |
AD
A049681

END
DATE
FILMED
3-78
DDC

(12)

Office of Naval Research

Contract N00014-76-C-0060 NR 064-478

Technical Report No. 32

DYNAMIC PHOTOELASTIC AND DYNAMIC FINITE ELEMENT ANALYSES OF POLYCARBONATE DYNAMIC TEAR TEST SPECIMENS

see back page for 1473

by

S. Mall, A.S. Kobayashi and Y. Urabe

January 1978

The research reported in this technical report was made possible through support extended to the Department of Mechanical Engineering, University of Washington, by the Office of Naval Research under Contract N00014-76-C-0060 NR 064-478. Reproduction in whole or in part is permitted for any purpose of the United States Government.

Department of Mechanical Engineering
College of Engineering
University of Washington

DYNAMIC PHOTOELASTIC AND DYNAMIC FINITE ELEMENT ANALYSES OF POLYCARBONATE DYNAMIC TEAR TEST SPECIMENS

by

S. Mall, A.S. Kobayashi and Y. Urabe*
Department of Mechanical Engineering
University of Washington
Seattle, Washington 98195

ABSTRACT

Dynamic photoelasticity and dynamic finite element methods were used to study dynamic responses of dynamic tear test (DTT) specimens of a ductile material, i.e. 3.2 mm (1/8 in.) thick polycarbonate sheets. Dynamic photoelastic patterns before and after the onset of unstable fracture showed that the dynamic fracture initiation toughness, K_{Id}, was attained during the second maximum load in the hammer load-time history and was approximately 65 percent of the fracture toughness, K_{IC}. Also dynamic stress intensity factors before and after crack propagation computed by dynamic finite element method using experimentally determined hammer load-time history were in reasonable agreement with those obtained from dynamic photoelasticity. The computed dynamic stress intensity factor prior to crack propagation was also in excellent agreement with the static stress intensity factors computed from dynamic strains adjacent to the crack tip.

INTRODUCTION

In a separate paper, dynamic photoelastic and dynamic finite element analyses were used to study the dynamic fracture response of dynamic tear test (DTT) specimens machined from a brittle photoelastic polymer, i.e. 9.5 mm

---

* Currently on leave from Takasago Technical Institute, Mitsubishi Heavy Industries, Takasago, Japan.

(3/8 in.) thick Homalite-100 plates [1]. The main objective of developing a DTT specimen as described in References [2-4] is to assess the brittle fracture response of a ductile material without requiring excessive specimen thickness or side grooving of the specimen. It stands to reason that similar dynamic photoelastic and dynamic finite element analyses should be conducted on a ductile photoelastic material where dynamic fracture responses different from those of the brittle Homalite-100 plates could be expected.

One such photoelastic material which is suitably transparent, ductile and relatively strain-rate insensitive is polycarbonate which has been used as a photoelastic-plastic model material by a number of investigators [5,6]. Polycarbonate flows under high stress, has a well-defined yield point of about 62 MPa (9000 psi) and exhibits a tensile instability phenomenon with accompanying Lueder's band. Although valid plane strain fracture toughness of this material is difficult to establish, it does exhibit cleavage fracture under high rate of loading and thus qualitatively models static and dynamic fracture of structural steel. As a result, polycarbonate sheets were used for dynamic photoelastic studies of DTT specimens in this investigation. In the following, the results of such dynamic photoelasticity and associated dynamic finite element analyses will be described.

Since much of the literature review on fracture toughness testing using DTT specimens as well as a review on the past dynamic photoelastic analysis of DTT specimens can be found in Reference [1], this paper will emphasize the experimental and numerical results of the polycarbonate DTT specimens.

POLYCARBONATE DTT SPECIMEN

The dynamic photoelasticity system and associated instrumentation are identical to those described in Reference [1]. Figure 1 shows the drop weight

tup and the four-arm strain gage bridge which was used to monitor the dynamic loading applied to the polycarbonate DTT specimen. The photoelastic model of the DTT specimen was identical in geometry except for its smaller thickness of 3.2 mm (1/8 inch) thickness as shown in Figure 1. Although a thicker polycarbonate sheet would have been preferred for simulating the plane strain state of stress in steel DTT specimens, the exceptionally high birefringence of polycarbonate resulted in crowding of isochromatic fringes in the vicinity of the crack tip and thus thinner specimens had to be used. From trial and error, the 3.2 mm thick polycarbonate was found to have the necessary optical sensitivity without buckling under the impact loading condition. Static fracture toughness tests of single-edged notch and compact tension specimens of this thin polycarbonate sheet showed significant plastic deformation and 100 percent shear lip in static fracture but a full thickness cleavage fracture was observed in DTT specimen under dynamic loading condition.

In the as-received condition, the polycarbonate sheet exhibited considerable residual stress distribution and thus the sheets were annealed after rough cutting. This annealing caused some distortion and shrinkage and thus the rough cut was made 25 mm (1 inch) over the actual specimen size. The annealing procedure consisted of overnight heating at 160°C, followed by a gradual cooling at the rate of 5°C per hour. During annealing, the polycarbonate sheet was tilted to about 5° over a glass sheet to prevent bubble formation between support glass and polycarbonate sheets. The starter crack consists of a 0.4 mm (.02 inch) wide edge crack of 25 mm (1 inch) length which was sawed and fatigued at an applied stress intensity factor of approximately 10 percent of its pop-in fracture toughness, K_{Ic}.

Static and dynamic material calibration tests were carried out to determine the stress-fringe constant, modulus of elasticity and Poisson's ratio at various

strain rates. A split Hopkinson bar system [7] with test bars of 3.2x9.5x254 mms and 3.2x9.5x381 mms was used for dynamic calibration. Results of these dynamic and static material properties are given in Table 1.

A valid plane strain fracture toughness could not be obtained in this thin sheet of polycarbonate since compact tension specimens with fatigued cracks exhibited ductile failure with gross yielding and necking. A fracture toughness associated with pop-in mode of polycarbonate was thus used following the procedure described in ASTM E-399 standards for a compact tension specimen with crack length of 19.05 mm (3/4 inch). Since the transparency of polycarbonate allowed observation of slow crack extension as well as pop-in crack extension during loading, a very small pop-in mode could be observed and the corresponding critical load was used to determine fracture toughness associated with this pop-in mode of crack extension using the expression given in ASTM E-399 [2] Results of this pop-in fracture toughness are also given in the table. Parvin and Williams [8] reported pop-in fracture toughness of 4 MPa$\sqrt{m}$ (3640 psi$\sqrt{in}$) and a crack initiation fracture toughness of 2.24 MPa$\sqrt{m}$ (2040 psi$\sqrt{in}$)for their single-edged notch and surface notch specimens of 3 mm (.12 inch) and 5 mm (.2 inch) thick polycarbonate specimens. The latter initiation fracture toughness was related to the curved crack front which occurred before pop-in fracture. No such phenomenon was observed in the pop-in failure mode of the compact tension specimen used in this analysis.

DYNAMIC FINITE ELEMENT ANALYSIS

The dynamic finite element algorithm used in this investigation is identical to that described in Reference [9]. Figure 1 also shows the finite element breakdown used in the plane stress analysis which was considered more appropriate because of the thinness of the specimen despite the cleavage fracture surface observed in DTT experiments.

DYNAMIC PHOTOELASTIC RESULTS

As shown in Figure 2, the dynamic photoelastic patterns of polycarbonate DTT specimens showed small scale plastic zone, r_y = .13-.38 mm (.005-.015 inches) preceding the running crack tip. This plastic zone, however, was not large enough to require an elasto-plastic analysis for the data reduction in the isochromatic fringe values. This small dynamic plastic zone, which is represented as a black head of the running crack tip, was in contrast to the significant net section yield and shear lip formation under static loading of polycarbonate compact specimens.

Figure 3 shows experimental data of dynamic stress intensity factor just prior to and after crack initiation as the crack propagated in seven polycarbonate DTT specimens with initially fatigued notch. A reasonably interpolated dynamic initiation fracture toughness, K_{Id}, from these experimental data would be 2.3 MPa$\sqrt{m}$ (2100 psi$\sqrt{in}$) with time to failure of about 1000 μsec. This K_{Id} value is approximately 65 percent of the pop-in static fracture toughness of 3.43 MPa$\sqrt{m}$ (3120 psi$\sqrt{in}$) described previously.

Figure 3 also shows that the dynamic fracture toughness (dynamic stress intensity factor), K_{ID}, decreased as the crack propagated in polycarbonate DTT specimen and is different from its counterpart of Homalite-100 DTT specimens which exhibited a maximum value in K_{ID} after crack propagation. Furthermore, Figure 3 shows increased fluctuations in K_{ID} as the crack propagated deeply in the initially compressive zone where K_{ID} decreased to about 50 percent of K_{Id}. This result indicates that should a minimum resistance to dynamic crack propagation, K_{Im}, exist, such K_{Im} would be considerably different from the fracture toughness, K_{Ic}, of this material.

All crack velocity data as a function of the specimen width are shown in Figure 4. The crack velocity decreased during the first 60% of the specimen

width and then remained nearly constant for the remaining width of the specimen. This variation in crack velocity in polycarbonate DTT specimens were different from those in Homalite-100 DTT specimens, where the crack velocity precipitously dropped at about 75% of the DTT specimen width. Crack velocity in the initially compressive zone of the polycarbonate DTT specimen was comparatively higher than its counterpart in Homalite-100 DTT specimen and the crack curved slightly at about 50% of width. In contrast, sharp crack curving was observed in the region of impact point of Homalite-100 DTT specimens.

Figure 5 shows the dynamic fracture toughness, K_{ID}, versus crack velocity for ductile polycarbonate specimen. The noticeable scatter in data could be due in part to the stress wave effects during dymamic loading. Although one can construct an averaged dynamic fracture toughness versus crack velocity relation of the proposed Γ-shape, such average curve was not fitted in due to large scatter of data in the present analysis.

RESULTS OF DYNAMIC FINITE ELEMENT ANALYSIS

Figures 6 and 7 show recorded impact load-time history for two polycarbonate specimens Nos. S090776-P and S100876-P. This impact load-time history was estimated from signals of a strain gage bridge placed 50 mm (2-1/2 in.) above the tup and should be considered only as an approximation of the true load-time history seen by the DTT specimen. In retrospect, a more precise measurement of the impact load could have been obtained by placing a piezo-electric transducer between the tup and the DTT specimen. For finite element analysis, the estimated load-time traces were idealized with straight line segments as shown in these two figures. In addition, the load time trace was retarded 10 μseconds to account for the stress wave propagation time from the average strain gage location to the tup tip. Crack tip position as a function time along with the interpolated crack initiation

time are also shown in Figures 6 and 7 for these two specimens.

Figures 8 and 9 show the dynamic stress intensity factor obtained from dynamic photoelasticity and dynamic finite element analysis in polycarbonate DTT specimen Nos. S090776-P and S100876-P. The large discrepancies between the measured and calculated dynamic stress intensity factors could be attributed to the not-so-precise determination of the load-time histories as well as the lack of viscous damping in the elasto-dynamic numerical analysis of polycarbonate specimens. Obviously a fine tuning of the impact load history would have reduced the discrepancies but limited computer resources precluded such additional effort.

Figures 10 and 11 show the development of numerical dynamic stress intensity factors from the start of impact to crack initiation in the two DTT specimen Nos. S090776-P and S100876-P. The experimental dynamic stress intensity factor along with computed dynamic stress intensity factor obtained at two locations in the crack tip region as per Loss' procedure [3] are also shown. Fair agreement was found between the experimental and numerical dynamic stress intensity factor.

The computed K_{Id} from the dynamic strains at two locations near the crack tip as per Loss' procedure [3] is in excellent agreement with the K_{Id} obtained directly from dynamic finite element analysis. Furthermore, comparisons of Figures 9 and 10 of polycarbonate DTT specimens with corresponding results for DTT specimens of Homalite-100 [1] show that the strain gage location near the crack tip for computing K_{Id} by Loss' procedure would be almost the same in both the ductile polycarbonate and the brittle Homalite-100 specimen in spite of the difference of thickness, material properties, impact load-time history and more importantly, the crack initiation time after impact.

DISCUSSION

The primary objective of dynamic tear test (DTT) and other impact tests such as Charpy and Izod impact tests is the determination of the total energy absorbed to fracture the specimen. In the latter two impact tests, unlike the DTT results, the energy absorbed up to fracture initiation cannot be measured directly. As a result, the total work done to specimen has been used to qualitatively characterize the fracture resistance of Charpy and Izod impact specimens. In order to provide further insight into the distribution of various energies in Charpy and Izod specimens, the computed values of external work, total strain energy, total kinetic energy and fracture energy for the two DTT specimens Nos. S090776-P and S100876-P are plotted in Figures 12 and 13. These figures show kinetic and fracture energies, at times close to complete crack penetrations, of the two polycarbonate DTT specimens are 50-65% and 25-35% of the external works. The unusually high amount of kinetic energy absorbed during dynamic tear test thus cast doubts on the significance of the total external work as a measure of fracture resistance of ductile material.

CONCLUSIONS

1. Dynamic fracture toughness at the onset of fracture, K_{Id}, of polycarbonate DTT specimens was about 65 percent of K_{IC} associated with pop-in.
2. Dynamic fracture toughness, K_{ID}, during crack propagation in the polycarbonate DTT specimens decreased to about 50 percent of K_{IC}.
3. Dynamic stress intensity factors determined from dynamic finite element analysis directly and indirectly using Loss' procedure were in excellent agreement with each other.
4. Kinetic energy represents a significant portion of the total external work in a ductile DTT-type specimen.

ACKNOWLEDGEMENTS

The results of this investigation were obtained in a research contract funded by the Office of Naval Research under Contract No. N00014-76-C-0600 NR064-478. The authors wish to acknowledge the support and encouragement of Drs. N. Perrone and N. Basdagas of ONR during the course of this investigation.

Table 1

AVERAGE MECHANICAL AND OPTICAL PROPERTIES OF POLYCARBONATE

E_S GPa (ksi)	2.38 (345)
E_D GPa (ksi)	2.72 (395)
ν_S	0.36
ν_D	0.36
f_{σ_S} MPa-mm/fringe (psi-in/fringe)	7.2 (41)
f_{σ_D} MPa-mm/fringe (psi-in/fringe)	6.7 (38)
ρ kg-sec^2/m^4 (lb-sec^2/in^4)	22 (0.000112)
c_1 m/sec (in/sec)	1960 (77,000)
c_2 (m/sec (in/sec)	910 (36,000)
c_p m/sec (in/sec)	1620 (63,600)
K_{Ic} * kPa$\sqrt{m}$ (psi$\sqrt{in}$)	3430 (3,120)

*Fracture toughness associated with pop-in mode.

NOTE: (i) Subscript S is for static properties
Average strain rate was 1.8×10^{-3} strain/sec

(ii) Subscript D is for dynamic properties
Average strain rate was 60 strain/sec

(iii) E, ν, f_σ and ρ are modulus of elasticity, Poisson's ratio, material stress-optic coefficient and density, respectively.

(iv) c_1, c_2 and c_p are dilatational, distortional and plate wave velocity, respectively.

REFERENCES

1. Mall, S., Kobayashi, A.S. and Urabe, Y., "Dynamic Photoelastic and Dynamic Finite Element Analyses of Dynamic Tear Test Specimens," submitted for publication in Experimental Mechanics.

2. "Standard Method of Test for Plane-Strain Fracture Toughness of Metallic Materials, E399-74", Book of ASTM Standards, Part 31, ASTM, Philadelphia, Pennsylvania, 1974.

3. Loss, F.J., "Dynamic Fracture Toughness of Reactor Pressure Vessel Steels," presented at the International Experts Meeting on Elastic-Plastic Fracture Mechanics, San Francisco, June 24-25, 1976.

4. "Method for 5/8 Inch Dynamic Tear Testing of Metallic Materials," MIL-STD-1601 (SHIPS), 8 May 1973.

5. Brinson, H.F., "Ductile Fracture of Polycarbonate", Experimental Mechanics, Vol. 10, No. 2, 1970, pp. 72-77.

6. Whitfield, J.K., "Characteristics of Polycarbonate as a Photo-elastic-Plastic Material", Ph.D. Thesis, Virginia Polytechnic Institute, 1969.

7. Bradley, W.B. and Kobayashi, A.S., "An Investigation of Propagating Cracks by Dynamic Photoelasticity", Experimental Mechanics, Vol. 10, No. 3, March 1970, pp. 106-113.

8. Parvin, M. and Williams, J.G., "Ductile-Brittle Fracture Transitions in Polycarbonate", Int. J. Fracture, Vol. 11, No. 6, December 1975, pp. 963-972.

9. Kobayashi, A.S., Mall, S., Urabe, Y. and Emery, A.F., "A Numerical Dynamic Fracture Analysis of Three Wedge-Loaded DCB Specimens", Proc. of the International Conference on Numerical Analysis in Fracture Mechanics, University College of Swansea, Jan. 9-13, 1978.

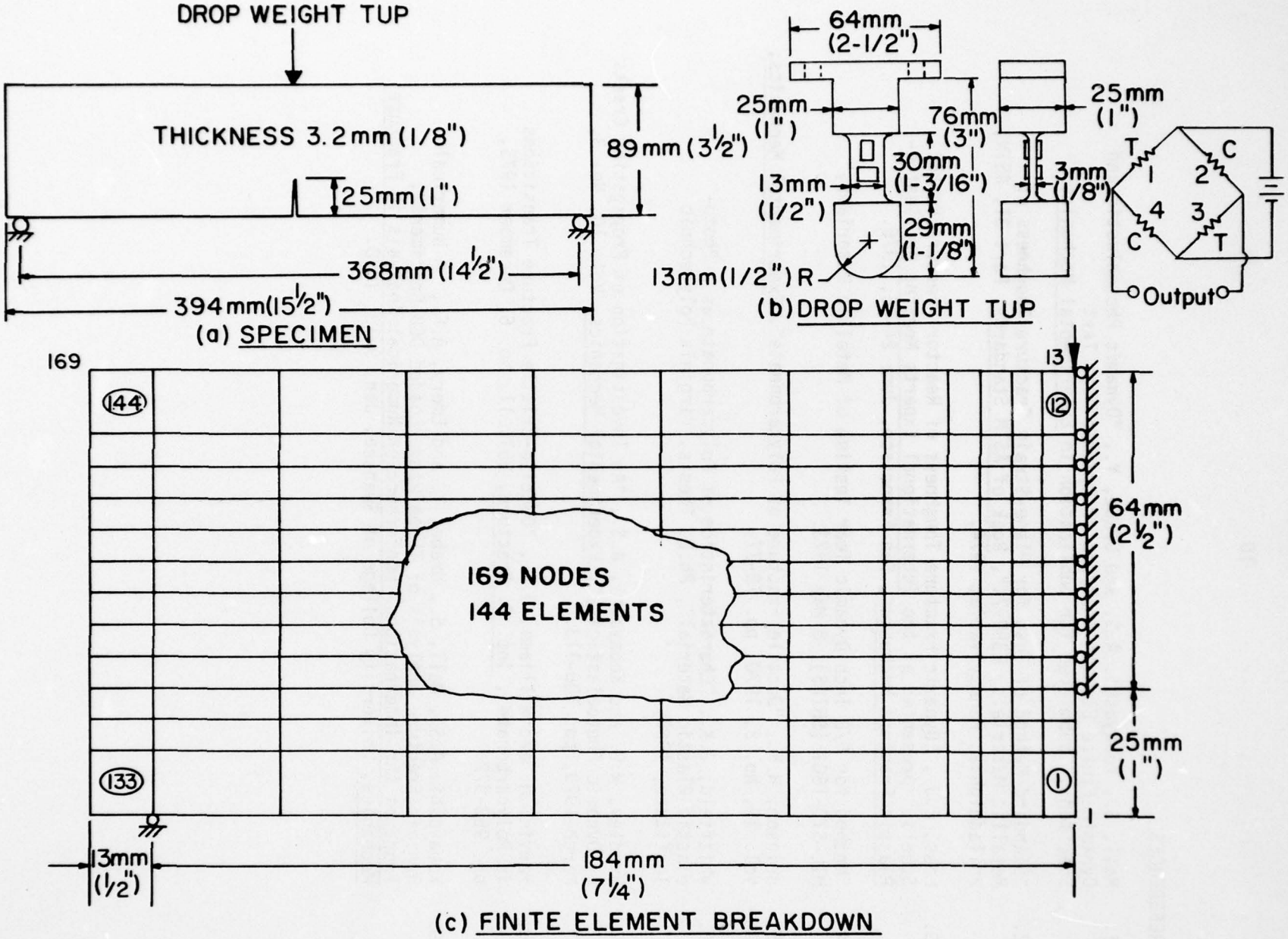

FIGURE 1. DYNAMIC TEAR TEST (DTT) SPECIMEN

(a) 6TH FRAME 126 μ SECONDS

(b) 12TH FRAME 282 μ SECONDS

FIGURE 2. TYPICAL DYNAMIC PHOTOELASTIC PATTERNS IN POLYCARBONATE DTT SPECIMEN NO. S101276-P.

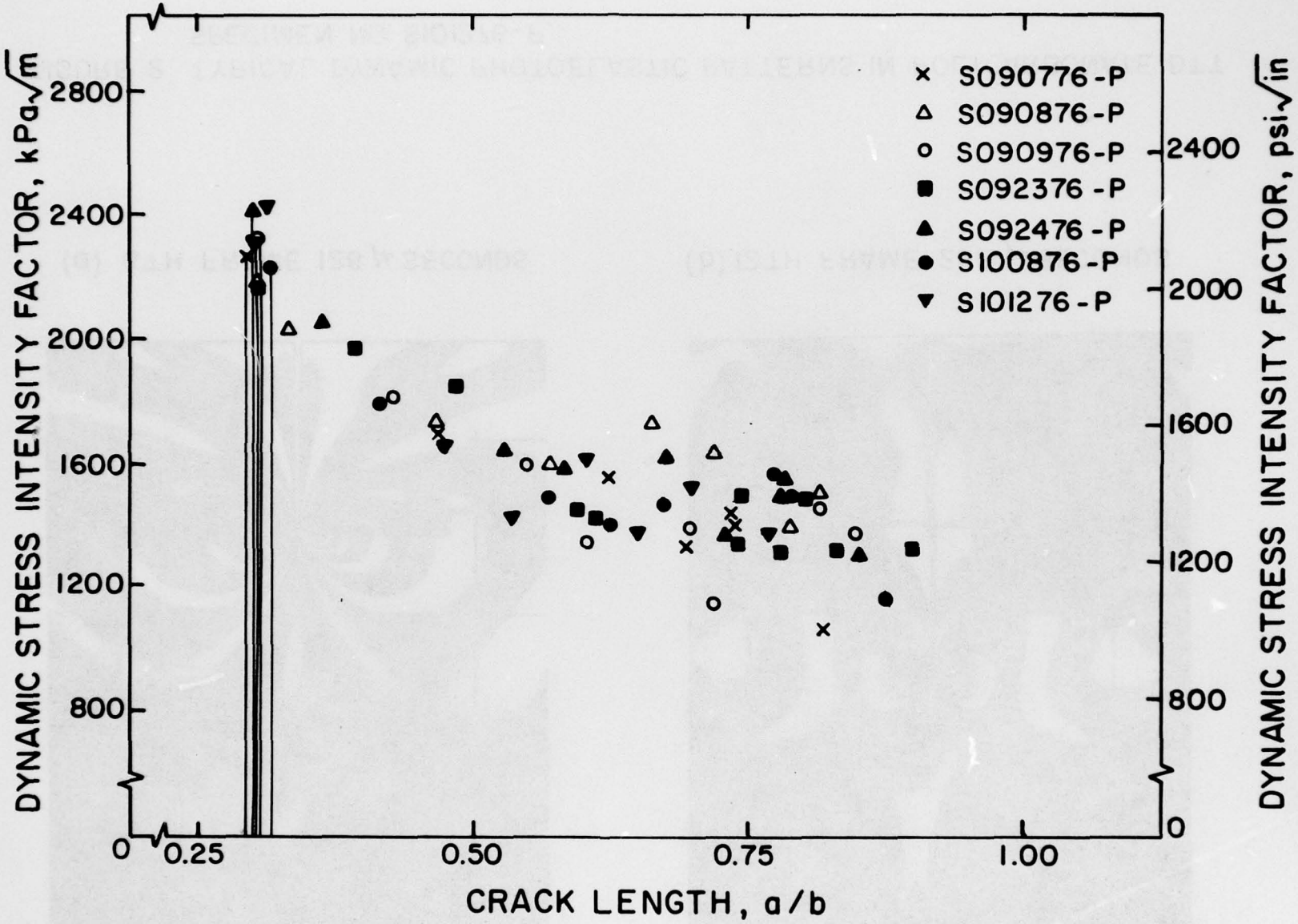

FIGURE 3. MEASURED DYNAMIC STRESS INTENSITY FACTORS BEFORE AND AFTER CRACK INITIATION IN SEVEN POLYCARBONATE DTT SPECIMENS.

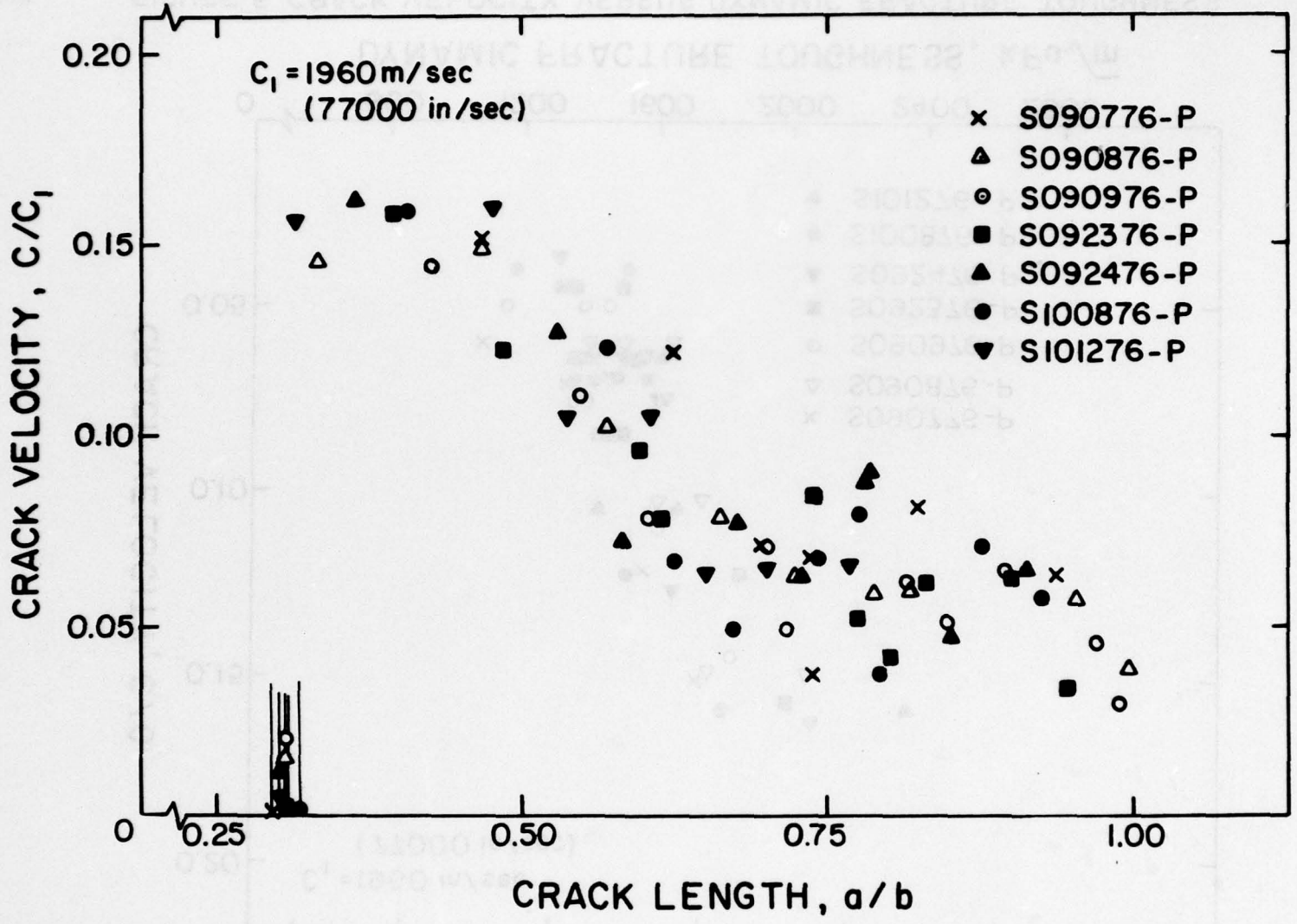

FIGURE 4. CRACK VELOCITIES IN SEVEN POLYCARBONATE DTT SPECIMEN

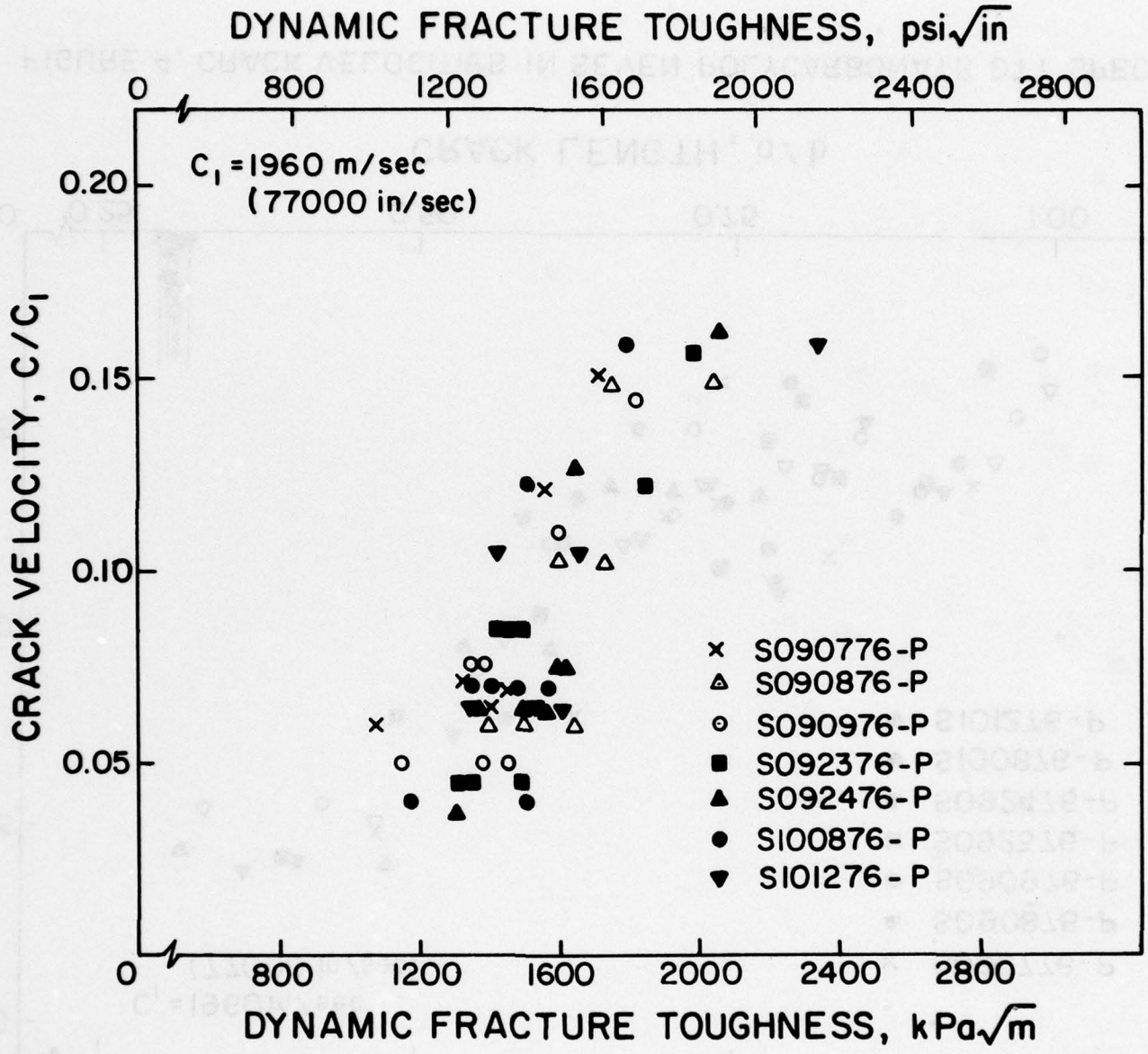

FIGURE 5. CRACK VELOCITY VERSUS DYNAMIC FRACTURE TOUGHNESS RELATION OF POLYCARBONATE DTT SPECIMENS.

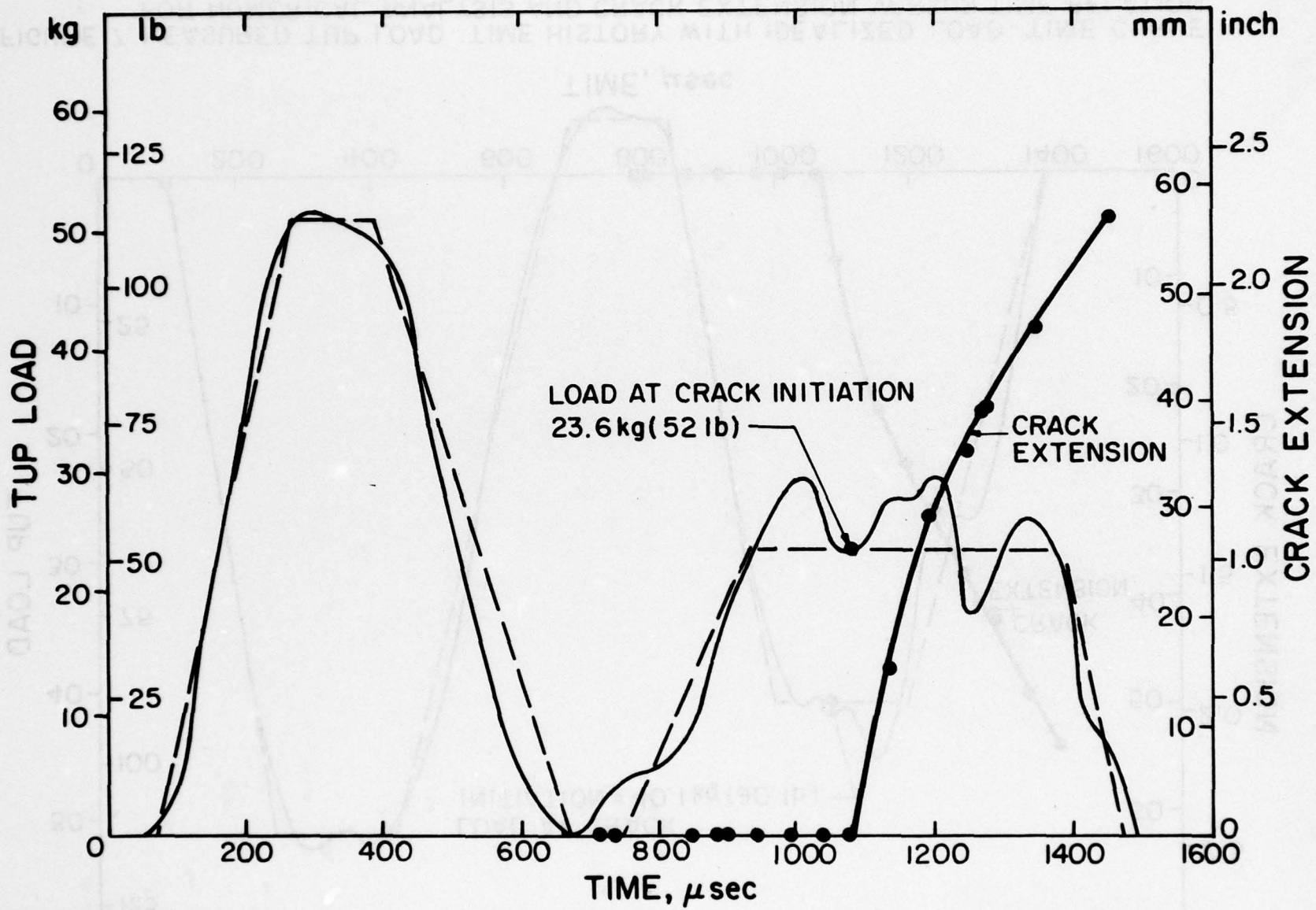

FIGURE 6. MEASURED TUP LOAD-TIME HISTORY WITH IDEALIZED LOAD-TIME CURVE FOR NUMERICAL ANALYSIS AND CRACK EXTENSION VERSUS TIME RELATION IN DTT TEST NO. S090776-P.

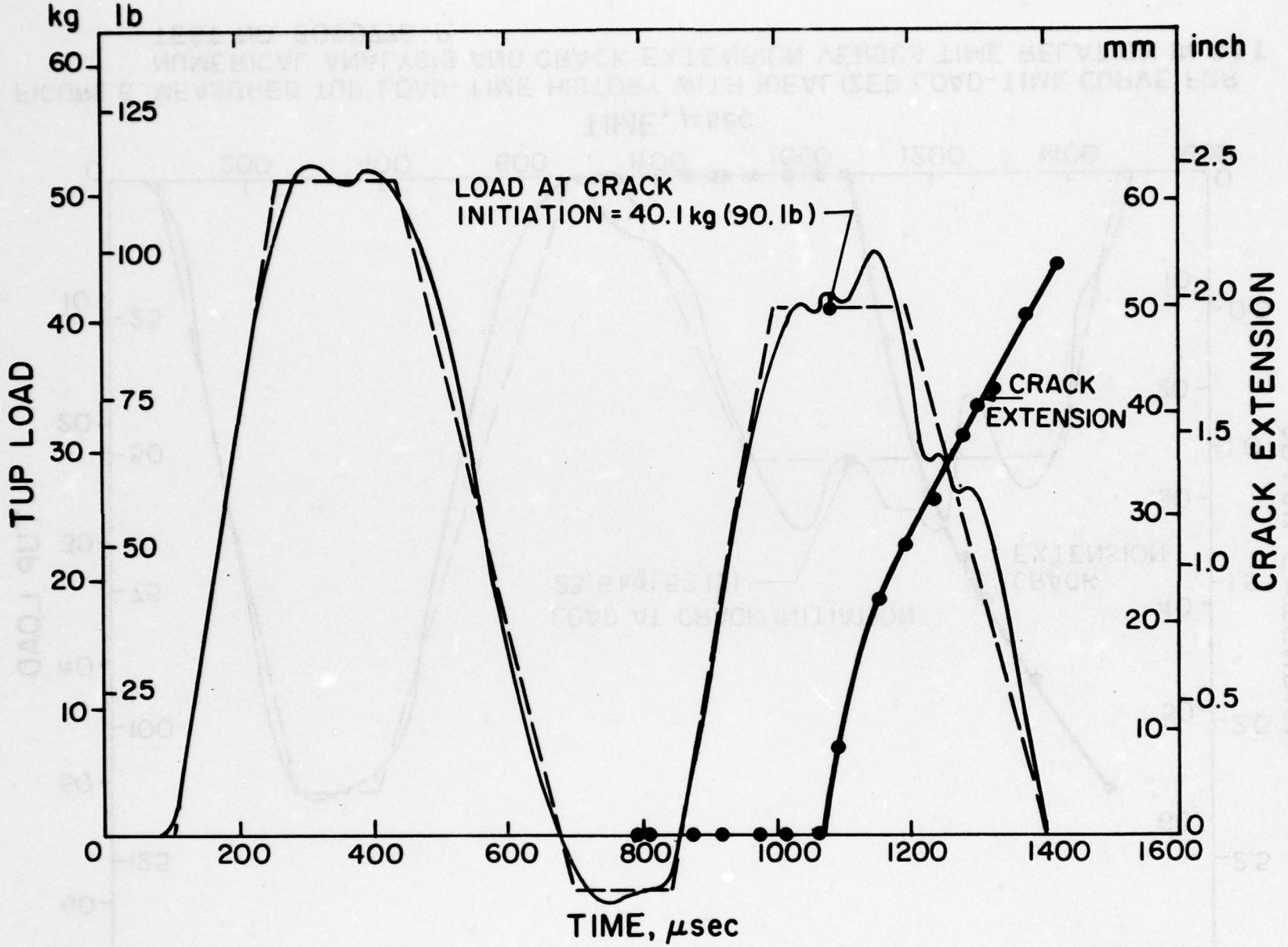

FIGURE 7. MEASURED TUP LOAD - TIME HISTORY WITH IDEALIZED LOAD - TIME CURVE FOR NUMERICAL ANALYSIS AND CRACK EXTENSION VERSUS TIME RELATION IN DTT TEST NO. S100876 - P.

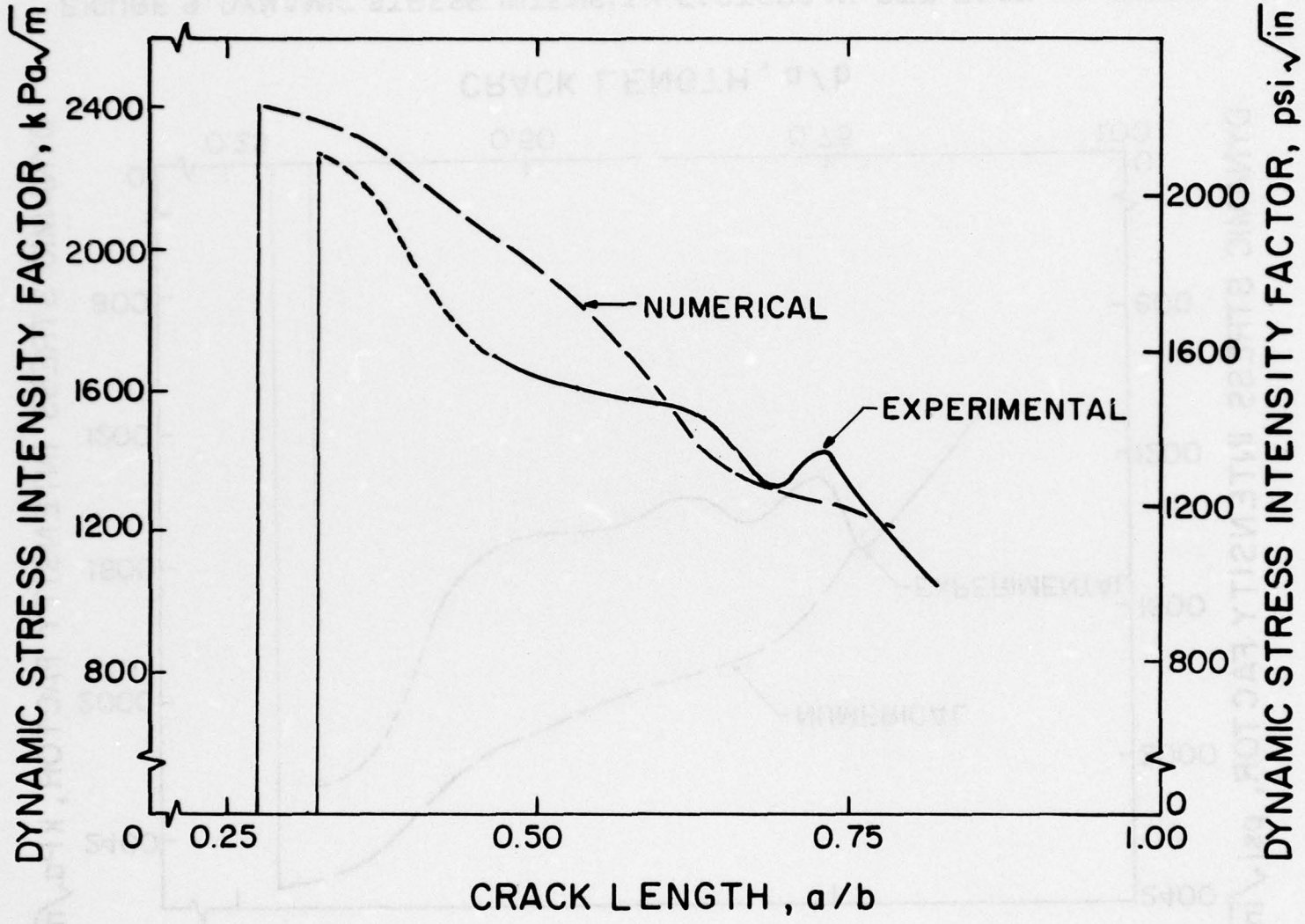

FIGURE 8. DYNAMIC STRESS INTENSITY FACTORS IN DTT TEST NO. S090776-P.

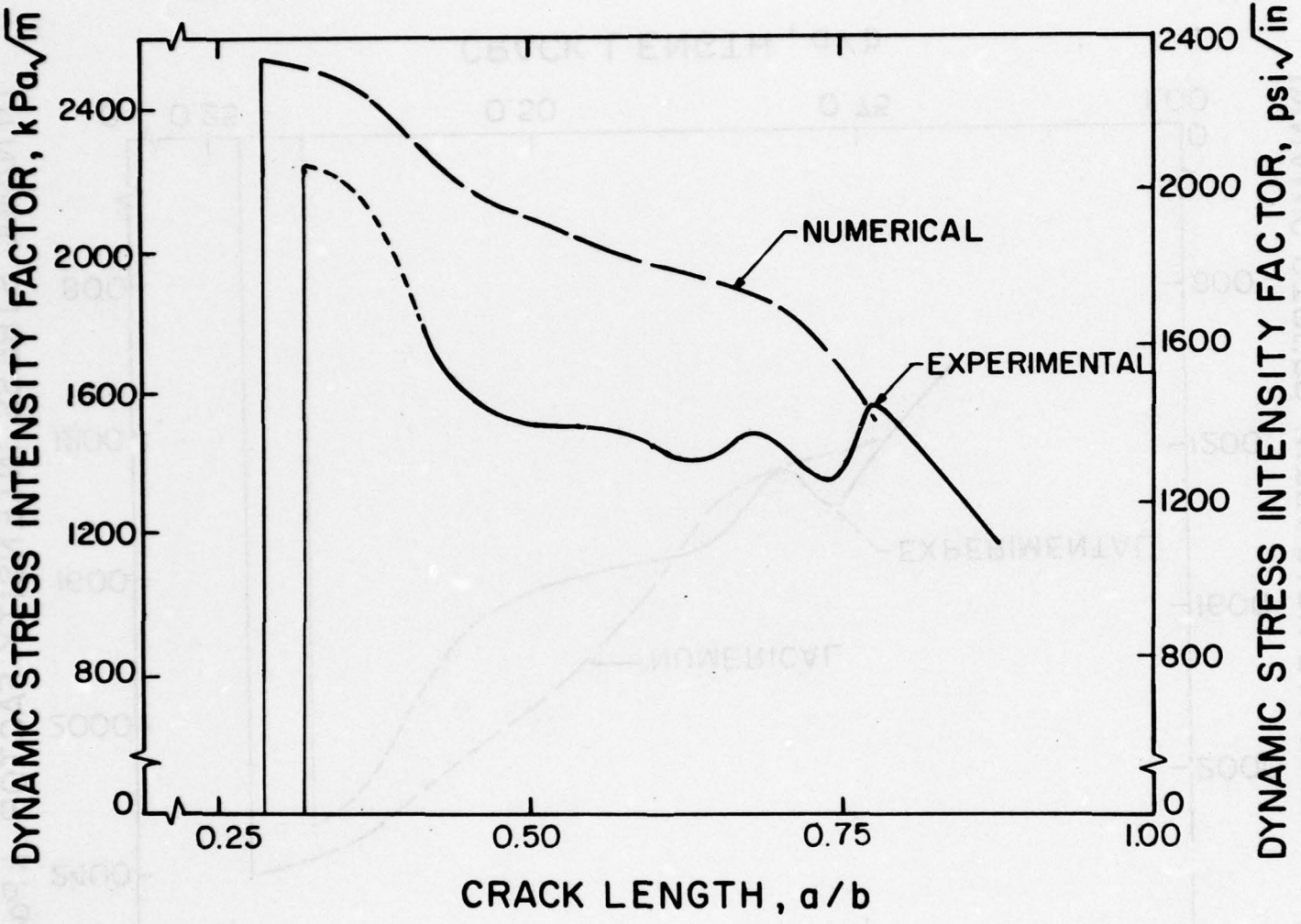

FIGURE 9. DYNAMIC STRESS INTENSITY FACTORS IN DTT TEST NO. S100876-P.

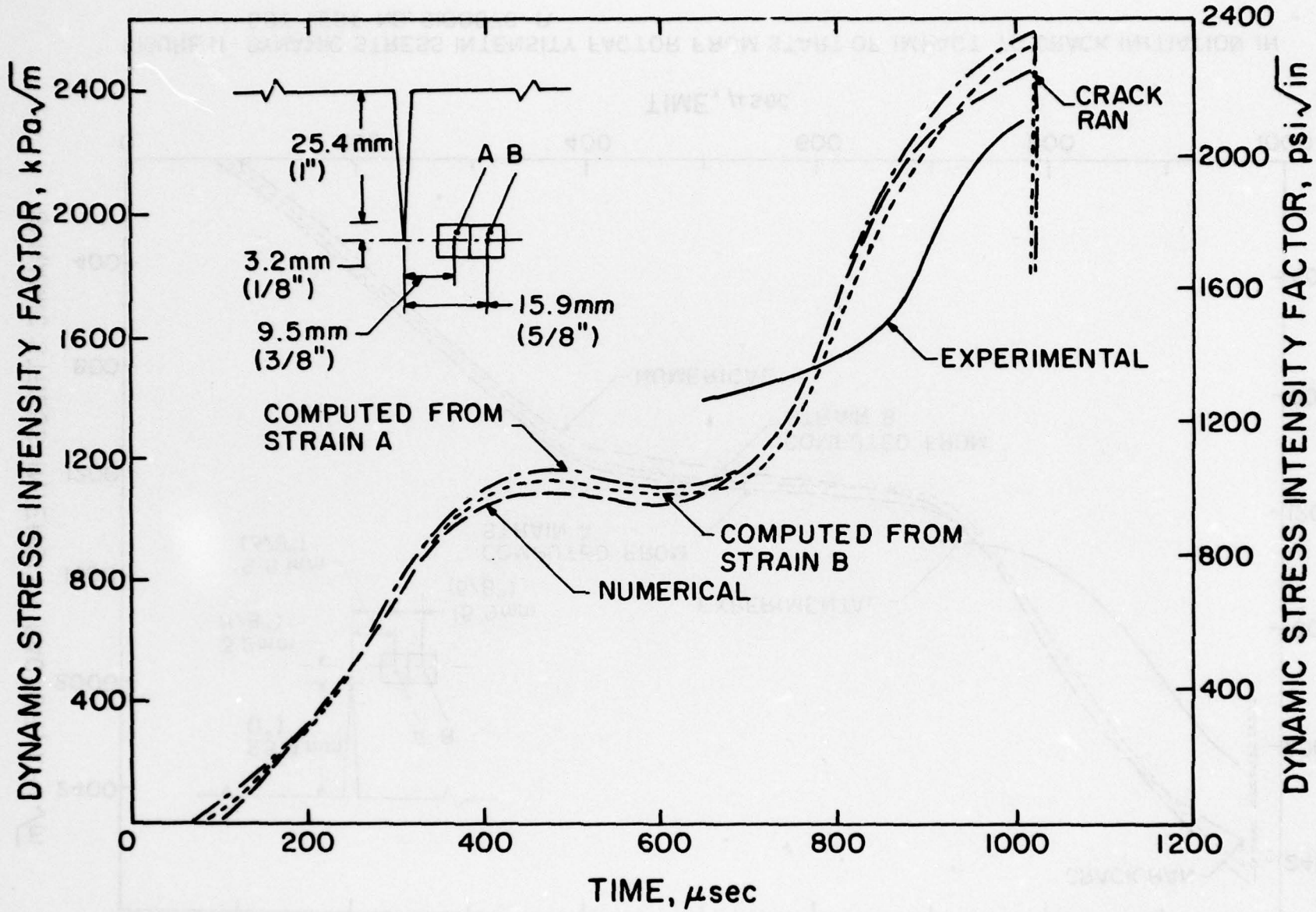

FIGURE 10. DYNAMIC STRESS INTENSITY FACTOR FROM START OF IMPACT TO CRACK INITIATION IN DTT TEST NO. S090776-P.

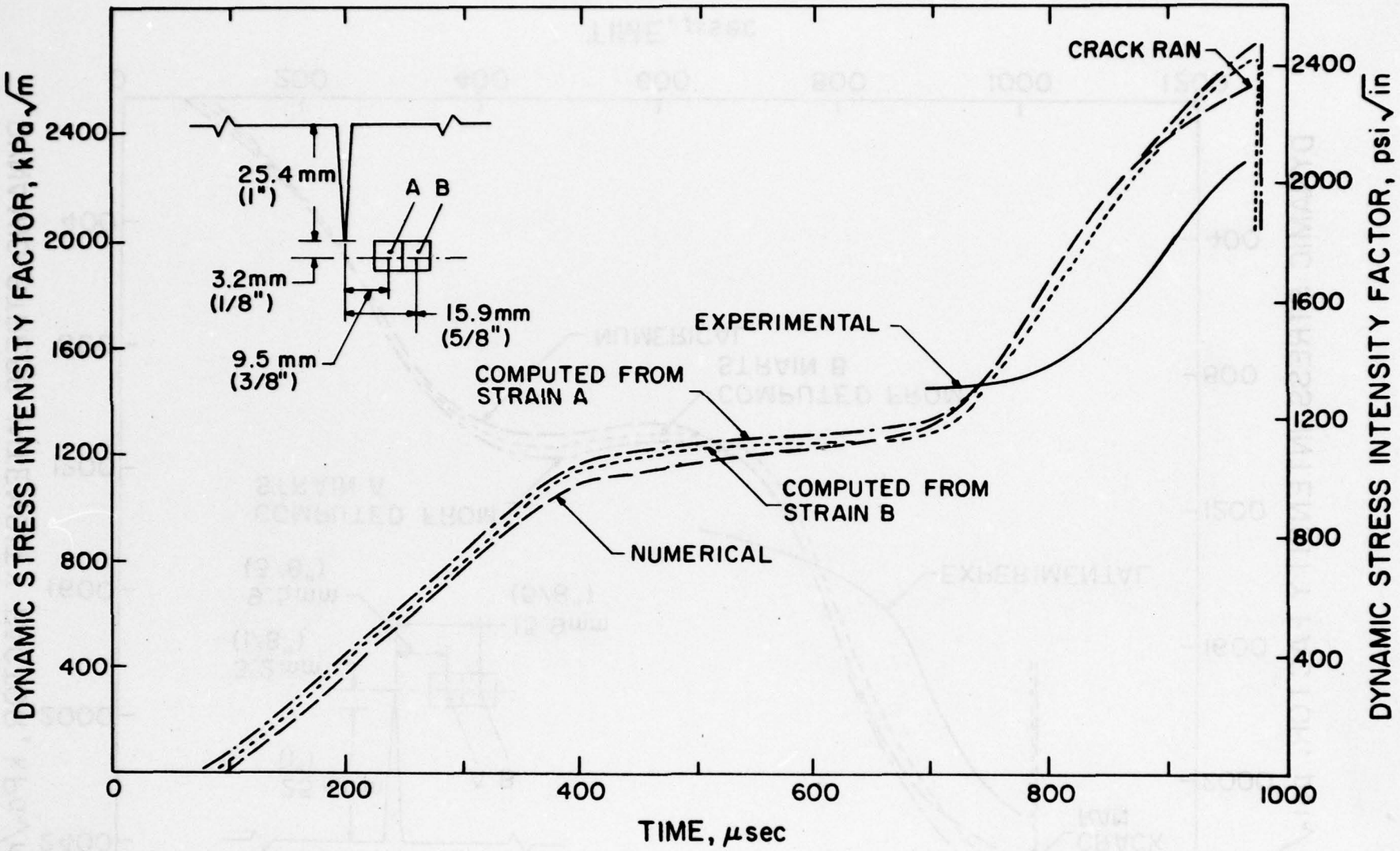

FIGURE 11. DYNAMIC STRESS INTENSITY FACTOR FROM START OF IMPACT TO CRACK INITIATION IN DDT TEST NO. S100876-P.

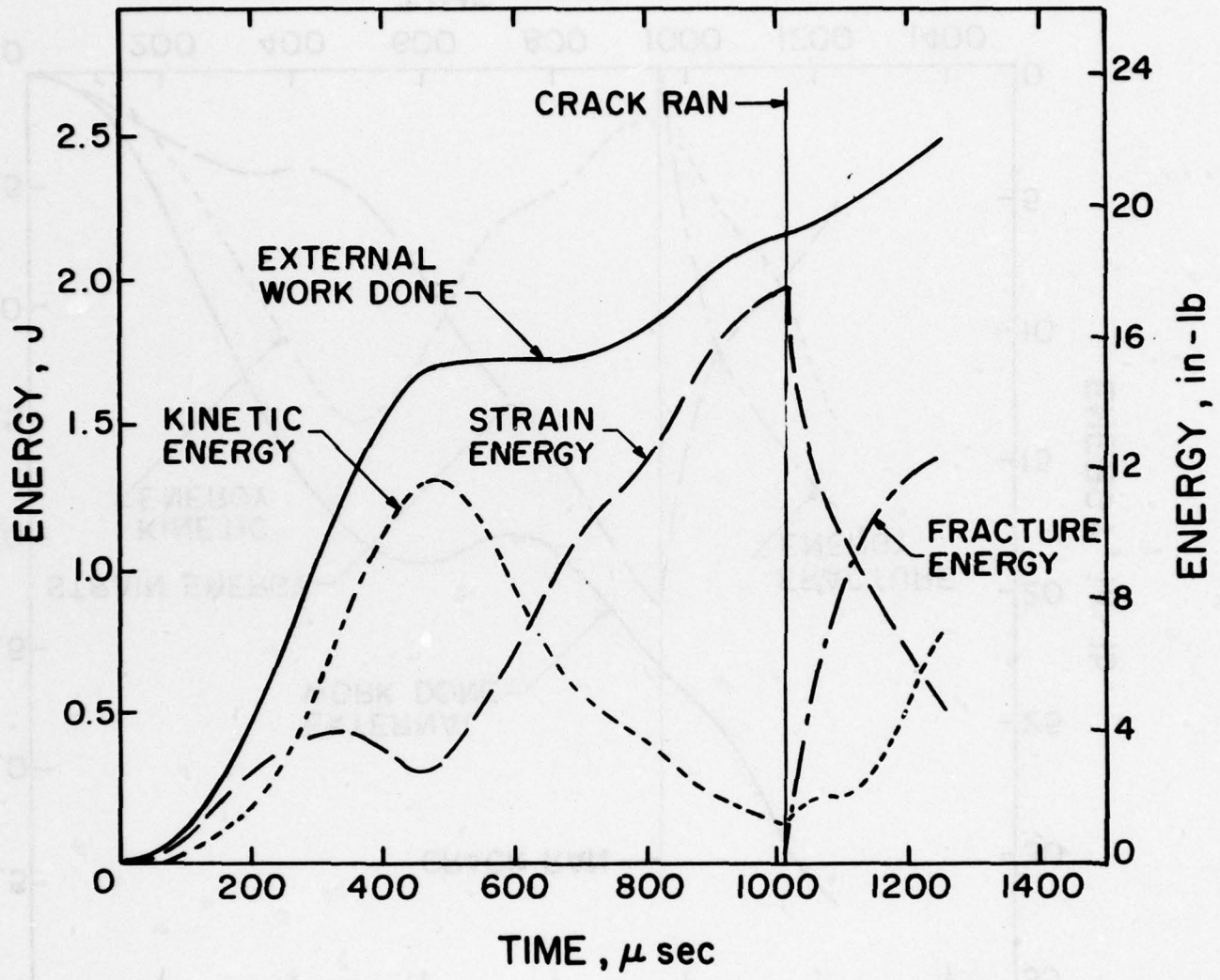

FIGURE 12. COMPUTED ENERGIES IN DTT TEST NO. S090776-P.

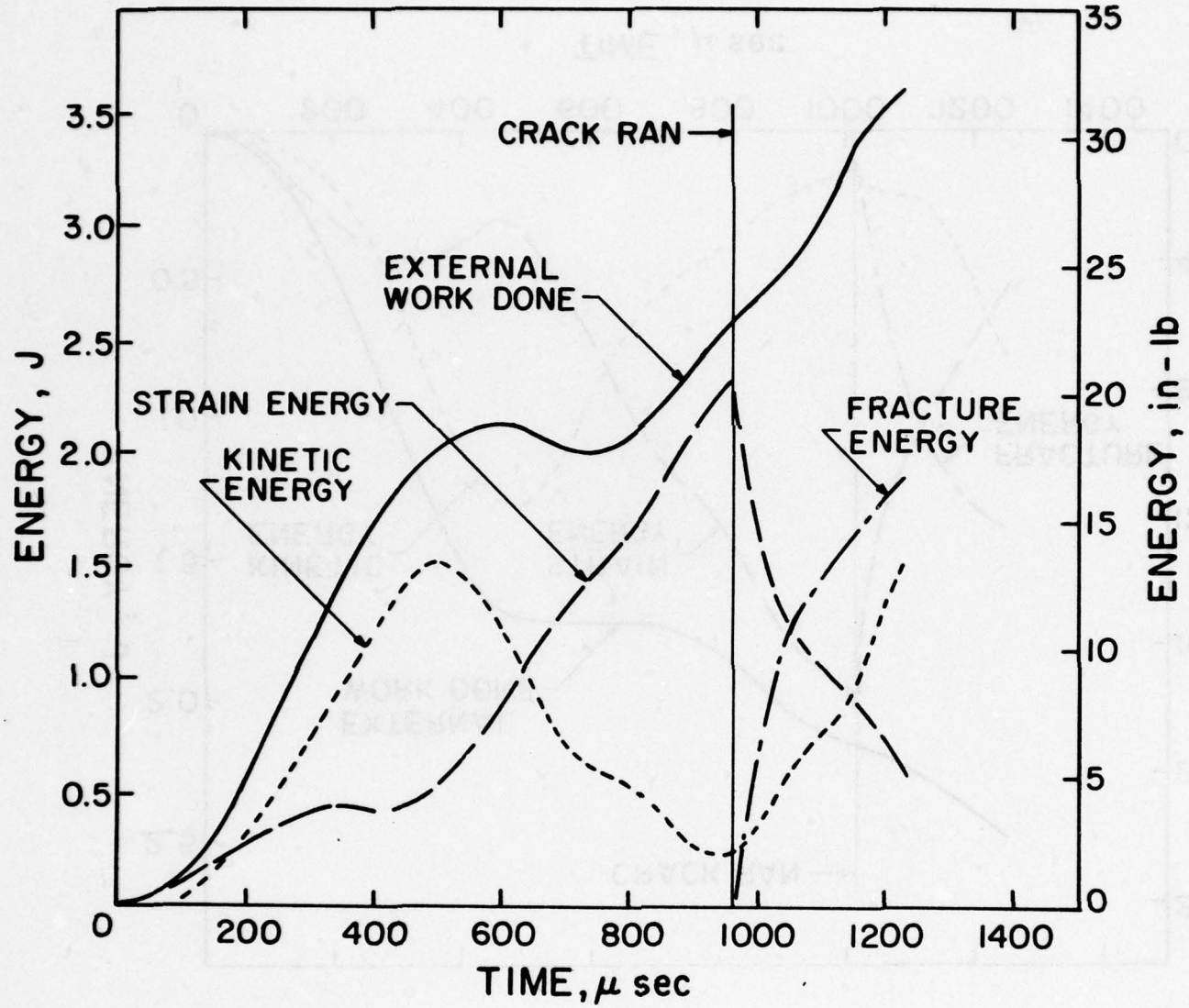

FIGURE 13. COMPUTED ENERGIES IN DTT TEST NO. S100876-P.

Unclassified

SECURITY CLASSIFICATION OF THIS PAGE (When Data Entered)

REPORT DOCUMENTATION PAGE

READ INSTRUCTIONS BEFORE COMPLETING FORM

1. REPORT NUMBER: TR-32	2. GOVT ACCESSION NO.
3. RECIPIENT'S CATALOG NUMBER	
4. TITLE (and Subtitle): Dynamic Photoelasticity and Dynamic Finite Element Analyses of Polycarbonate Dynamic Tear Test Specimens.	5. TYPE OF REPORT & PERIOD COVERED: Interim Report.
	6. PERFORMING ORG. REPORT NUMBER: 32
7. AUTHOR(s): S./Mall, A.S./Kobayashi [redacted] Y./Urabe	8. CONTRACT OR GRANT NUMBER(s): N00014-76-C-0060 NR 064-478
9. PERFORMING ORGANIZATION NAME AND ADDRESS: University of Washington, Department of Mechanical Engineering, Seattle, Washington 98195	10. PROGRAM ELEMENT, PROJECT, TASK AREA & WORK UNIT NUMBERS
11. CONTROLLING OFFICE NAME AND ADDRESS: Office of Naval Research, Arlington, Virginia	12. REPORT DATE: Jan [redacted] 78 13. NUMBER OF PAGES: 23 (12) 26p.
14. MONITORING AGENCY NAME & ADDRESS (if different from Controlling Office)	15. SECURITY CLASS. (of this report): Unclassified 15a. DECLASSIFICATION/DOWNGRADING SCHEDULE

16. DISTRIBUTION STATEMENT (of this Report)

Unlimited

DISTRIBUTION STATEMENT A
Approved for public release;
Distribution Unlimited

17. DISTRIBUTION STATEMENT (of the abstract entered in Block 20, if different from Report)

18. SUPPLEMENTARY NOTES

19. KEY WORDS (Continue on reverse side if necessary and identify by block number)

Fracture Mechanics, Fracture Dynamics, Crack Propagation, Crack Arrest, Finite Element Analysis, Dynamic Photoelasticity

20. ABSTRACT (Continue on reverse side if necessary and identify by block number)

Dynamic photoelasticity and dynamic finite element methods were used to study dynamic responses of dynamic tear test (DTT) specimens of a ductile material, i e. 3.2 mm (1/8 in.) thick polycarbonate sheets. Dymamic photoelastic patterns before and after the onset of unstable fracture showed that the dynamic fracture initiation toughness, K_{Id}, was attained during the second maximum load in the hammer load-time history and was approximately 65 percent of the fracture toughness, K_{IC}. Also dynamic stress intensity factors (continued on reverse)

over

DD FORM 1 JAN 73 1473 EDITION OF 1 NOV 65 IS OBSOLETE S/N 0102-014-6601

Unclassified

SECURITY CLASSIFICATION OF THIS PAGE (When Data Entered)

K SUB IC K SUB Id

400 344

before and after crack propagation computed by dynamic finite element method using experimentally determined hammer load-time history were in reasonable agreement with those obtained from dynamic photoelasticity. The computed dynamic stress intensity factor prior to crack propagation was also in excellent agreement with the static stress intensity factors computed from dynamic strains adjacent to the crack tip.